Milda Pociūtė-Adomavičienė,
***Anne Schwarz,**
Sigitas Stanys

Kaunas University of Technology,
Faculty of Design and Technologies,
Department of Textile Technology,
Studentų 56, LT-51424, Kaunas, Lithuania,
E-mail: milda.pociute@stud.ktu.lt

***Ghent University,**
Department of Textiles
Technologiepark 9, 9052 Gent (Zwijnaarde)
E-mail: Anne.Schwarz@UGent.be

Analysis of the Wetting Behaviour of an Inclined Fibre

Abstract
The surfaces of physical bodies are the subject of fascinating research, which combines different scientific disciplines, such as physics, chemistry and material science. A physical body's surface properties determine its wettability, among other things. The wetting of solid planes has been quite well understood in scientific terms for centuries. Nonetheless, the wetting properties of cylindrical bodies (e.g. fibres), which are the objects of research in the present work, may differ significantly from those of plane surfaces, because the wetting of cylindrical bodies exhibits some unique features due to their inherent curvature. Whilst the study of liquid film instability on fibres was first studied by Lord Rayleigh in the second half of the 19th century, and has been analysed further by numerous researchers over recent decades, there is still a lack of literature on the complete understanding of the factors that drive liquid instability, due to the immense complexity of break-down mechanisms. It is evident that a more detailed study of liquid film instability process is needed. No evaluation of the behaviour of liquid on fibre, which is inclined at different angles, has been found in the literature either. This research aims to add greater understanding to the processes that take place when a fibre is coated by a fluid. In particular, we investigate the instability of a glycerol film on a motionless polyamide 6 fibre after withdrawing it at varying inclination angles from a liquid (glycerol) reservoir. The results showed that liquid behaviour is to a certain degree influenced by the inclination angle of a fibre.

Key words: *wettability, instability, Rayleigh wavelength, contact angle.*

Introduction

Fibre wetting is of great importance in many fields, including fibre coating (applying dyes, finishes, etc.), the production of composite materials (adhesion between fibres and resin binders) and many other areas. When it is desired that liquid should penetrate a fabric, the liquid must wet single filaments first. If the garments are intended to be water-repellent, then the liquid should not coat single fibres. In all these cases, we are dealing with fibres (assuming they are cylindrical bodies, as is in fact the case when we are dealing with synthetic fibres). We set forward the hypothesis that liquid behaviour on a horizontally-oriented fibre might differ from its behaviour on an inclined one. Thus in this paper we present our investigation into the behaviour of liquid on fibres which are inclined at different angles.

The theory of wettability has been studied intensively over recent decades and is quite well understood in scientific terms [1 - 5]. When a droplet is put on a solid surface, many different physical and chemical properties of both the solid and the liquid phase influence the fluid's dynamics, such as surface tension, density and temperature of both liquid and solid, viscosity of liquid, surface roughness and shape of the solid [6].

By definition [7], wettability is the tendency of a fluid to spread on and preferentially adhere to or 'wet' a solid surface in the presence of other immiscible fluids. In other words, liquids are able to form an interface with solids.

From a macroscopic point of view, the interface between a liquid and its vapour is defined by a change of density. Thus interfaces are often considered as thin membranes and places of special, two-dimensional conditions and phenomena, such as interfacial or surface energy, specific adsorption, mass transfer, heterogeneous catalysis, the Marangoni effect and electric double layer, etc. [6].

Molecules at the surface of two different phases differ energetically from the ones in the bulk of each phase; this is because the intramolecular forces in the bulk of each phase differ from those acting between the particles at the interface of two phases (e.g. forces acting in between liquid-liquid or liquid-solid phases).

Let us first consider two immiscible fluids (see Figure 1). Here, it is well seen that the attractive forces between molecules of two liquid phases are substantially smaller than those between molecules of the same phase. This results in an interfacial tension.

The molecules of two phases are subjected to cohesion forces that keep them united. In the case of a particle that is situated at the surface, the sum of these cohesion forces is directed towards the bulk, resulting in a cohesion pressure. However, intermolecular or adhesive forces also exist, and these adhere the molecules of one liquid to the molecules of the other liquid that they contact [8].

In the case of liquid and solid phases meeting each other, we can say that liquid tends to repel at the surface if the forces of adhesion are smaller compared to those of cohesion. On the other hand, liquid spreads on the surface of the solid, when the forces of adhesion are greater than the forces of cohesion. A thin film of the liquid will form on the solid surface in which long-range forces are present (usually only van der Waals' forces are taken into account) [9].

Disjoining pressure

A thin liquid film in sub-microscopic scale has a thickness of *e*, which results from

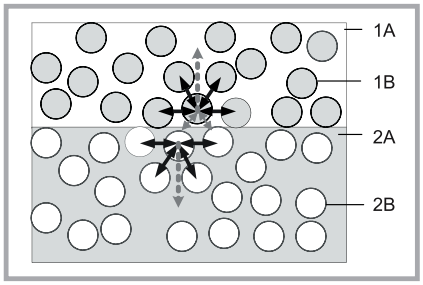

Figure 1. *Forces acting in the bulk and at the interface of two phases:1A - liquid phase1, 1B - molecule of liquid 1, 2A - liquid phase 2, 2B - molecule of phase 2, ◄► shows cohesion forces between molecules, - - ► shows the sum of cohesion forces, ◄► shows adhesion forces.*

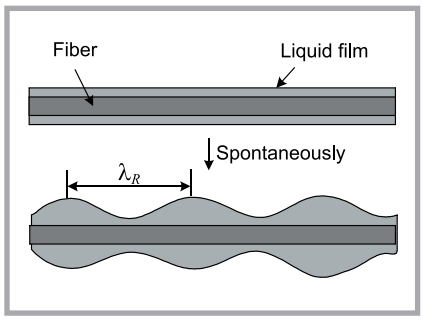

***Figure 2**. Liquid film instability.*

competition between the long-range forces. The attractive potential of the interaction of long-range forces acting between two atoms or molecules decreases with intermolecular distance r_i as r_i^{-6}. When this potential is integrated over all pairwise interactions between two half-spaces separated by a distance e, one finds [9]:

$$P(e) = \frac{A}{12\pi \cdot e^2} \tag{1}$$

where A is a solid-liquid Hamaker constant assumed to be either positive or negative between two physical bodies, depending on their polarisation.

Another parameter $\Pi_d(e)$ indicates the disjoining pressure, which can be defined as the pressure that must be brought up to keep the film on a solid at a constant thickness. Long-range forces are expressed in terms of disjoining pressure $\Pi_d(e)$ and can be derived from $P(e)$ [9]:

$$\Pi_d(e) = -\frac{dP}{de} \tag{2}$$

Laplace pressure

So far, the forces acting at liquid-solid interfacial area have been discussed. Now we shall consider the situation in the liquid film which is sufficiently far away from the solid-liquid interfacial region where the disjoining pressure is absent.

At the liquid-air interface, the cohesion forces inside the liquid are stronger than the adhesion forces with the air phase. The liquid will tend to minimise its surface area, because it is energetically favourable for molecules to be surrounded by other molecules of the same origin. Thus, the liquid will try to reach the state of minimum energy and the liquid film will start to undulate. In a curved liquid surface, there exists a pressure difference between the inside and the outside of the surface. Laplace's law relates the pressure difference across a liquid film sphere to the tension in the film.

$$\Delta p = \gamma\left(\frac{1}{R_1} + \frac{1}{R_2}\right) \tag{3}$$

where Δp is the difference between the internal and external pressures at the surface, γ is a surface tension of the liquid, and R_1 and R_2 are the two main radii of curvature.

Disjoining and Laplace pressure

If we coat a fibre of radius r with a liquid film having a uniform thickness e_0 (see Figure 2), the interface spontaneously begins to undulate, and highly curved regions with crests and troughs are formed. This results in a formation of an array of uniformly distributed droplets. The equilibrium configuration of a system is determined by the competition between Laplace pressure and disjoining pressure.

The film spontaneously breaks up into small droplets at regular intervals when the acting Laplace pressure is greater than the disjoining pressure.

Plateau & Rayleigh [9] indicated that a liquid film of radius e_0, subjected to a disturbance of periodicity λ, becomes unstable due to the surface tensions, and breaks up into droplets if λ is greater than $2\pi\, e_0$.

The distance between single drops can be calculated using Rayleigh's equation:

$$\lambda_R = 2.88\ \pi\ r_0 \tag{4}$$

where r_0 is an initial radius of the column 'fibre-liquid film'. It has to be noted that this formula takes neither the different properties of liquids and fibres nor their interactions into account [9, 10].

In the scheme presented in Figure 3, the situation after film rupture is represented.

The longitudinal view of a droplet of a fluid dwelling on a fibre is illustrated. $h(z)$ represents the liquid-air interface profile. Outside the droplet, where $|z| \to \infty$, a thin, homogenous film of thickness e still coats the fibre. The parameter h_0 indicates the sum of fibre radius b and film thickness e. The two radii of curvature are indicated as R_1 and R_2 respectively. The parameter L_W characterises the droplet length. The system is rotationally symmetric around the fibre axis z, and can also be mirrored on the droplet height axis h. The dashed line $a(z)$ describes the reference shape in the form of a half-sphere and is determined by

$$a(z = 0) = h(z = 0);$$

this means that it contacts the surface profile of the liquid-air interface h(z) at the apex P'. In this osculation point P', the slope and the bend of the actual surface $h(z)$ and the reference surface $a(z)$ are identical.

The apparent contact angle θ is described by the intersection of the spherically-shaped surface $a(z)$ and the thin liquid film e.

In the literature, two different approaches to calculating the apparent contact angle can be found.

Neimark [12] derived a formula for apparent contact angle in dependence on the droplet height h, the radius b of the fibre and the radius of the curvature R_0 at the top [11]:

$$\cos\theta = \frac{b+h}{b} - \frac{(b+h)^2 - b^2}{2b}\left[\frac{1}{b+h} + \frac{1}{R_0}\right] = 1 - \frac{h(b+h)\cdot(2b+h) - R_0 h^2}{2bR_0(b+h)} \tag{5}$$

Bauer and Dietrich [13] expressed the apparent contact angle by including the

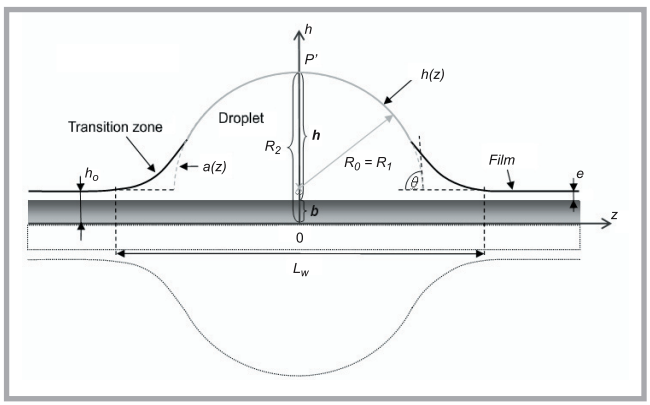

***Figure 3.** Schematic profile of a droplet [11]; h(z) - liquid-air interface profile, e - film thicknes outside the droplet, h_o - sum of fibre radius b and film thickness e, R_1 and R_2 - radic of droplet's curvatures, L_W - droplet length, z - fibre axis, h - droplet height axis, a(z) - reference shape, P' - apex.*

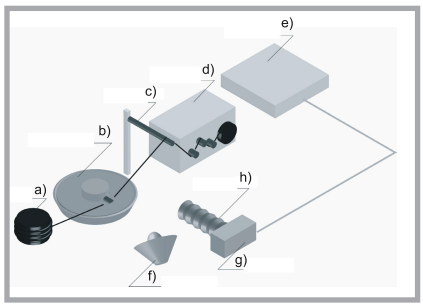

Figure 4. *Experimental setup for fibre coating; a) yarn supply, b) liquid reservoir, c) adjusting unit, d) winding unit, e) computer, f) cold light source, g) digital camera, h) stereo microscope.*

initial film thickness e_0 in equation (5), and obtained the following result:

$$\cos\theta = \frac{b+h}{b+e_0} + \frac{(b+h)^2-(b+e_0)^2}{2(b+e_0)}\left[\frac{1}{b+h}+\frac{1}{R_0}\right] \quad (6)$$

Much experimental and theoretical effort has been directed towards understanding and explaining the multitude of factors that govern the wetting of solid bodies. Moreover, numerous studies of the shape and spreading of droplets deposited on cylindrical substrates have been published [9, 13 - 18]. However, knowledge is still lacking, especially regarding the case of Rayleigh instability when fibres are withdrawn from a liquid reservoir. Efforts are constantly being made by researchers to bring more light into the field of liquid film instability on curved substrates. For instance, Kamath et al. [18] derived an expression for the time to the total breakdown of a liquid film. To draw another example, Quéré, Di Meglio and Brochard-Wyart [9] analysed the Rayleigh instability of liquid films coating fibres with regard to its prevention, and discovered that a liquid film will be stable when its thickness is in the range of 100 Å.

Besides the studies mentioned, no work could be found dealing with liquid film instability on thin fibres (fibre radius in the range of 100 μm) with respect to the influence of fibre orientation; such studies as have been published only consider horizontally- and vertically-arranged fibres.

Beyond this background, the present work evaluates the instability of liquid films that coat fibres, and investigates the influence of varying inclination angle on liquid film instability.

Materials and test methods

Polyamide 6 fibre was chosen as the test material; this was a finish-free smooth monofilament, and had a circular cross-section with a radius of 100 μm. We chose glycerol (propane-1,2,3-triol, sometimes called Glycyl alcohol) as the test liquid on the basis of a list of references [19 - 23, etc.] showing that alcohols, especially glycerol, are often used in experiments that deal with the wetting properties of textile materials.

A computer-based imaging system was used to monitor the interaction of liquids with fibrous material. The computer-based imaging system (see Figure 4) consists of a digital camera (Nikon Coolpix 4500) connected to a stereoscopic zoom microscope (Nikon SMZ 800), a computer, a light source (cold light, in order to avoid any influence of heat on the test liquid), a liquid reservoir, an adjusting unit for the inclination angle and a winding unit.

A special computer program was used to display images on the computer screen.

The polyamide 6 fibre was unwound from the yarn supply unit, passed through a liquid reservoir containing the test liquid, guided over an inclination angle adjusting system, and wound onto a rotating cylinder.

The stereo microscope was situated in such a way that it could focus on the coated fibre immediately after it was pulled out of the liquid reservoir. The speed at which the filament was drawn through the liquid reservoir was maintained at 0.003 m/s in order to result in a uniformly thin annular film, and to be able to compare the results.

When the fibre was uniformly coated by the liquid, the winding unit was stopped and the dynamic process of liquid film breaking into an array of droplets was recorded. For each inclination angle, twenty records from a side view were made. Twenty different inclination angles were adjusted, ranging from 0° to 90° at an interval of 5°. The liquid in the liquid reservoir was exchanged after each time in order to prevent changes in the viscosity of the test liquid.

The records were captured as images. The initial film thickness as well as the development of instability was then evaluated using the Lucia image analysis system (version 5.0). As well as the measurements of initial film thickness and wavelength between neighbouring droplets, we were also able to measure the characterising parameters of droplet profile, namely the radius of droplet curvature and the droplet height. These parameters provide the basis for calculations of the Rayleigh wavelength and the contact angle that the liquid droplet forms on the fibre.

Results and discussion

Initial film thickness

Having captured the moment when the liquid film on the surface of the fibre was formed, it was possible to measure its initial thickness (see Figure 5). As the diameter of the filament was known (200 μm), the initial film thickness was obtained as follows: from the diameter of the column 'fibre-glycerol', the diameter of the filament was subtracted and the obtained value dimidiated.

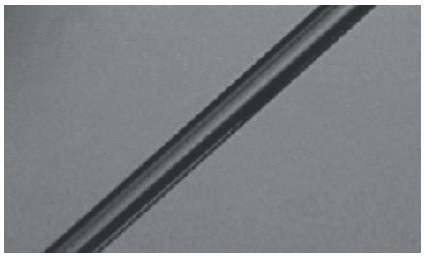

Figure 5. *Initial film thickness of glycerol film on fibre inclined at 45°.*

Table 1. *Mean values and coefficients of variation of initial thickness of glycerol film.*

Inclination angle, °	Initial film thickness, μm	Coefficient of variation, %
0	16±2	9.6
5	17±2	10.0
10	17±1	7.5
15	19±2	8.0
20	19±2	9.7
25	24±2	6.3
30	24±3	10.0
35	25±3	10.0
40	26±3	10.1
45	24±3	10.9
50	13±2	15.1
55	23±3	15.0
60	21±3	14.1
65	23±2	9.8
70	25±4	15.1
75	26±1	4.7
80	26±3	13.0
85	28±4	14.3
90	37±2	5.3

As the unevenness of the filament diameter varied only within the range of 0.4%, it was assumed that those changes have no significant influence on the measurements of initial film thickness. Table 1 displays the mean values of the initial thickness of the glycerol film for the 20 different inclination angles, as well as the coefficients of variation. On average 20 records were made for each inclination angle to obtain the representative data.

As it is difficult to see how the results change in Table 1, the mean values and the trend-line of the initial thickness' dependence on the inclination angle are presented in Figure 6.

The linear trend-line shows that the initial film thickness slightly increases with the inclination angle, from 16 μm at the inclination angle of 0°, up to 28 μm when the inclination angle of a fibre is 85°. Only inclination angles of 50° and 90° differ from the main tendency in this set of experiments. The drop of initial film thickness in a former case is quite large (outside limits of errors); the increase of initial film thickness in the latter case is also quite large (also outside limits of errors). Such a comparatively thick film on a vertical fibre could be explained by a downward flow of liquid due to the gravity, whereas we still have no explanation for such a thin liquid film on a fibre being inclined at 50°. It might be caused by a certain critical angle being influenced by the orientation of the fibre-liquid system. More experiments should definitely be performed with other kind of liquids that may help to explain this phenomenon.

Break-down mechanism

The development of glycerol film instability proceeds in steps, as is shown in Figure 7. The process is documented with pictures numbered from (1) to (8). As soon as the fibre is entrained, a film of glycerol is formed around the fibre, as shown in picture (1). The film starts to undulate (2), and with time the amplitude of waves increases (3). Droplets form quickly and they are connected via a thin, annular film. This stage is depicted in (4). It can be observed that neighbouring droplets move towards each other (5). In doing so, the one droplet situated below the other droplet moves up the fibre, and the one drop positioned above the other slides downwards until they meet each other (6) and coalesce (7). This event occurs repeatedly until the droplets reach a certain distance from each other, as shown in (8).

We thus conclude that gravity forces do not play an essential role; although the meniscus of glycerin droplet is slightly deformed, some droplets move up the fibre (and not only downwards). This leads us to the conclusion that the greatest account is of the Laplace pressure which causes the joining of droplets.

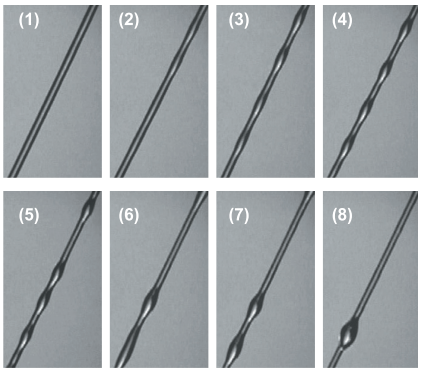

Figure 7. *Development of glycerol film instability on polyamide fibre inclined at 60°.*

Wavelength

The wavelengths measured between droplets are presented in Table 2. As it is difficult to see in which way the results change in Table 2, the mean values of the initial thickness are plotted versus the inclination angle in Figure 8.

In Figure 8 it is seen that the slope of the measured wavelength first increases at inclination angles from 0° to 15°. Yet, starting from an angle of 30°, the slope constantly decreases. The trend-line shows that the overall tendency is for a decrease in wavelength with an increase in inclination angle. This could be explained via a change in film thickness, which was increasing with the increase in inclination angle. As film becomes thicker, droplets form more easily; it is known that the formation of droplets

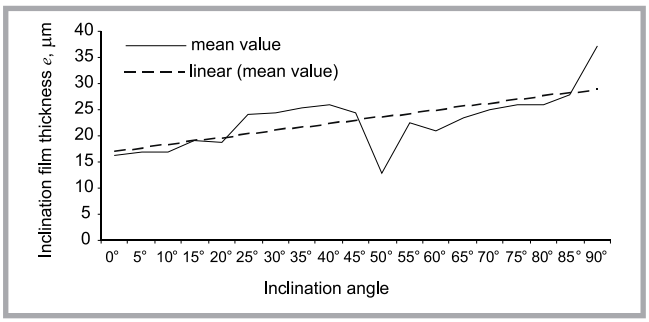

Figure 6. *Initial film thicknesses of glycerol film.*

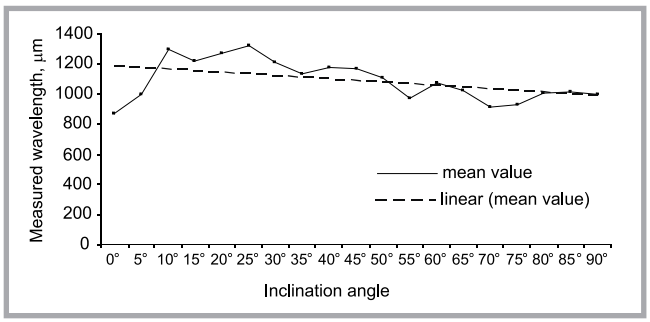

Figure 8. *Measured wavelengths of glycerol droplets.*

Table 2. *Mean values and coefficients of variation of wavelengths between droplets of Glycerol on a fiber.*

Inclination angle, °	0	5	10	15	20	25	30	35	40	45	50	55	60	65	70	75	80	85	90
Wavelenght, μm	868	999	1299	1224	1272	1321	1209	1138	1179	1167	1109	971	1072	1026	913	928	1007	1018	1002
Coefficient of variation, %	13.8	12.8	11.9	12.5	13.8	15.3	10.0	13.3	14.7	13.0	13.5	14.1	11.5	13.5	11.8	10.9	14.2	15.0	16.7

Table 3. *Calculated values of wavelengths between droplets according to Rayleigh.*

Inclination angle, °	0	5	10	15	20	25	30	35	40	45	50	55	60	65	70	75	80	85	90
Wavelength, μm	1088	1098	987	1072	1084	1145	1069	1051	1126	1125	995	1052	1069	1108	1030	1141	1051	1139	1087

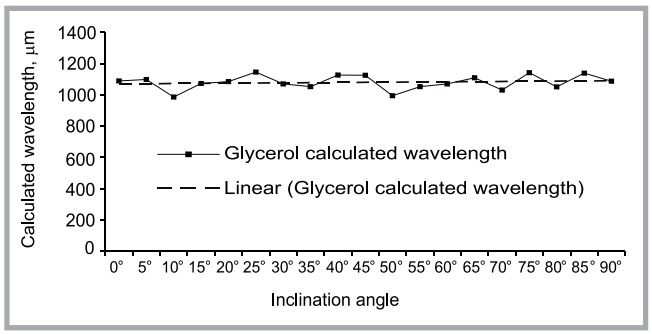

Figure 9. *Calculated wavelengths of glycerol droplets.*

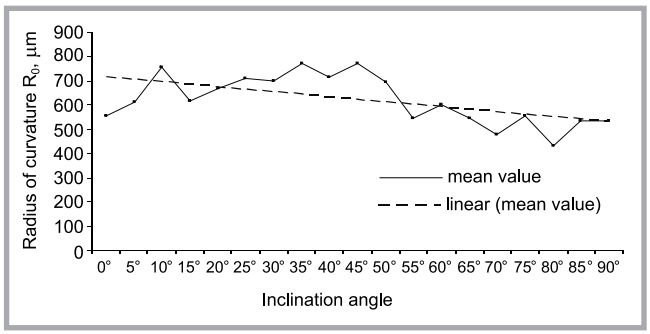

Figure 10. *Measured radii of curvature of glycerol droplets.*

Table 4. *Measured values and coefficients of variation of radii of curvature.*

Inclination angle, °	0	5	10	15	20	25	30	35	40	45	50	55	60	65	70	75	80	85	90
Mean value of curvature, µm	557	612	756	616	671	708	698	773	717	769	693	543	599	546	478	556	434	533	535
Coefficient of variation, %	16.6	14.2	12.4	16.0	14.7	15.1	14.7	11.4	16.7	10.8	16.4	14.1	15.6	15.0	13.6	14.6	15.6	15.6	14.4

might be avoided if the film thickness is extremely small (in the range of a few hundred angstroms). Gravity also plays a certain role here.

The values shown in Table 2 and Figure 8 were compared to the results obtained by applying the formula derived by Rayleigh (equation (4)) for the distance between neighbouring droplets (see Table 3). The results were found to approximately correlate.

From Figure 9, it is well seen that the calculated values are almost constant; the difference between them is just 154 µm, taking the value of 1141 µm at 75° as maximum and the value of 987 µm at 10° as minimum. This can be verified by the linear trend-line. Apparently, those calculations show that on the basis of the Rayleigh formula, the inclination angle has no influence on the distance of neighbouring droplets from each other.

The difference between the dependencies presented in Figure 8 (measured values) and in Figure 9 (theoretical values) is clearly visible. The compatibility between these two wavelengths should be analysed. However, at this stage of our research we first wanted to evaluate the influence of the fibre's indicated angle on the behaviour of the liquid which covers the fibre. In the near future we plan to investigate this relation. We also assume that using other test liquids would provide more information.

This investigation does not match the trend of changing the measured distance between single droplets residing on inclined fibres .

It is also well seen that the slopes of the calculated wavelength versus inclination angle show a better continuity compared to the slopes of the measured wavelength.

The radii of curvature (average values of at least 40 measurements) as measured for each inclination angle and the coefficients of variation are specified in the following Table 4. As it is difficult to see in which way the results change in Table 4, the mean values of the radii of curvature are plotted versus the inclination angle in Figure 10.

The trend-line apparently decreases with the increasing inclination angle of the fibre. This leads to the conclusion that the droplet profile is influenced by inclination angles.

The droplet height as measured for each inclination angle is almost constant (the slope of the trend-line increases only very slightly, and can be assumed to be constant, having a value of approximately 50 µm (the coefficient of variation varies from 5.93% to 12.85%). Obviously, the inclination angle of the monofilament has no impact on the droplet height.

The contact angle was calculated according to equations (5) and (6). The results are presented in Table 5.

It is evident that at inclination angles of 25°, 35°, 40° and 45°, the values calculated by equation (5) do not match with the experimentally observed values (see Figure 11).

When examining the images of the fibre-liquid system obtained for these angles, it is clearly visible that droplets are formed. Therefore, cos θ is expected to be lower than 1.

Conclusions

In this work we demonstrated that the inclination angle of the fibre can be de-

Table 5. *Calculated contact angles of droplets, resting on inclined fibers.*

Inclination angle, °	cos θ	cos θ	Contact angle, °
	According to equation 5	According to equation 6	
0	0.97	0.96	15.48
5	0.98	0.97	14.49
10	0.99	0.98	10.00
15	0.99	0.96	15.22
20	0.99	0.98	12.47
25	1.00	0.98	12.67
30	0.99	0.98	11.10
35	1.01	0.99	9.73
40	1.01	0.97	13.14
45	1.00	0.99	9.89
50	0.99	0.99	9.85
55	0.97	0.96	16.01
60	0.98	0.96	15.37
65	0.97	0.95	17.45
70	0.96	0.96	16.81
75	0.97	0.97	13.17
80	0.94	0.94	20.12
85	0.97	0.95	17.49
90°	0.97	0.96	16.49

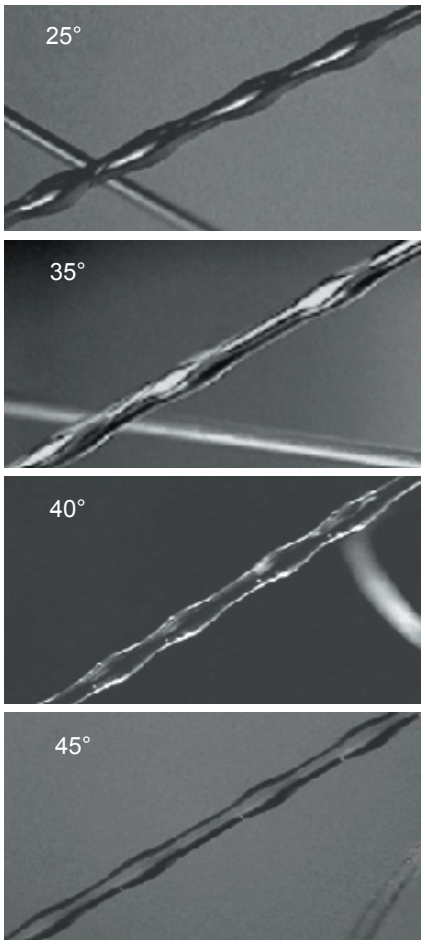

Figure 11. *glycerol film instability on monofilament inclined at 25°, 35°, 40° and 45°.*

scribed as one of the parameters of the liquid-fibre system that influence the development of liquid film instability.
Having investigated liquid film instability in dependence on the inclination angle of the fibre from both experiments and theoretical calculations, the specific findings are listed below;

Initial film thickness

The analysis showed that the initial film thickness of liquid slightly increases with the increase in the inclination angle of the fibre. Only at the inclination angle of 50° did we obtain a sudden drop in the initial thickness of a liquid film on a fibre. Thus this case will be of interest to us as we continue our research work.

Break-down mechanism

A visual investigation of the development of droplets on the polyamide 6 filament leads to the conclusion that the driving forces in this dynamic process are the Laplace and disjoining pressures. It was observed that even at high inclination angles, two droplets of glycerol coalesce by moving towards each other; one droplet moves up the fibre while the other one slides down. Apparently, the Laplace pressure accounts more for the joining of droplets than gravity does.

Wavelength

The work on the measurement of wavelength discovers that the values of calculated and measured wavelength between glycerol droplets correlate exceptionally well.

Contact angle

The comparison of the results of contact angles obtained by theoretical calculation was an important addition; this revealed that the formula derived by Neimark (equation 5), which does not take the initial thickness of the liquid film into consideration, is not in accordance with the observed contact angles on our fibre-liquid system. However, the formula derived by Bauer & Dietrich (equation 6), which includes the initial thickness of liquid film around the fibre, represents the apparent contact angle quite satisfactorily from a theoretical point of view. It would be advantageous to extend the examination of both theoretical formulas and, for Neimark's formula, to describe in a more general way when this formula will lead to incorrect values.

Acknowledgments

We would like to thank Prof. D. Lukáš from the Technical University of Liberec, Czech Republic, for his help in this and previous topics.

References

1. *Fukai, J., et al. 'Wetting Effects on the Spreading of a Liquid Droplet Colliding with a Flat Surface: Experiment and Modeling', Physical Fluids 7 (2), 1995, pp. 236 - 248.*
2. *Palasantzas, G., de Hosson, J.Th. M., 'Wetting of Rough Surfaces', Acta Mater 49, 2001, pp. 3533 - 33538.*
3. *Brochard-Wyart, F., Fondecave, R., 'Wetting Laws for Polymer Solutions', Europhysics Letter, 37 (2), 1997, pp. 115 - 120.*
4. *Heywood, D., 'Textile Finishing', Society of Dyers and Colourists, Textile and Chemical Consultant, Sacola Associates, Cheadle Hulme, UK, 2003, 137 - 148.*
5. *Bahr, M., 'Wetting and Capillary Flow of Surfactant Solutions and Inks', doctoral thesis, Lund University, Institute for Surface Chemistry, 2003, pp. 14 - 19.*
6. *Frohn, A., Roth, N., 'Dynamics of Droplets', Springer Verlag, Berlin, Heidelberg, New York, 2000, pp. 1 - 125.*
7. *Craig, F. F., 'The Reservoir Engineering Aspects of Waterflooding', Monograph Vol. 3 of the Henry L. Doherty Series, Society of Petroleum Engineers of AIME, 1971.*
8. *Fraunhofer Institut für Grenzflächen- und Bioverfahrenstechnik: http://www.igb.fraunhofer.de/WWW/GF/GrenzflMem/Grenzflaechen/en/what-is-an-interface.en.html.*
9. *Quéré, D., Meglio, J. M., Brochard–Wyart, F., 'Spreading of Liquids on Highly Curved Surfaces', Science, Vol. 249, 1990, pp.1256 - 1260.*
10. *Pociūtė, M., Adomavičius, K., Stanys, S., 'Liquid Film Instability on a Single Fibre', Materials Science (Medžiagotyra), ISSN 1392-1320, Vol. 11, No. 1, 2004, pp. 84 - 87.*
11. *Wagner, H. D., 'Spreading of Liquid Droplets on Cylindrical Surfaces: Accurate Determination of Contact Angle', Journal of Applied Physics, Vol. 67, No. 3, 1990, pp.1352 - 1355.*
12. *Neimark, A. V., 'Thermodynamic Equilibrium and Stability of Liquid Films and Droplets on Fibres', J. Adhesion Sci. Technol., Vol. 13, No. 10, 1999, pp.1137 - 1154.*
13. *Bauer, C., Dietrich, S., 'Shapes, Contact Angles, and Line Tensions of Droplets on Cylinders', Physical Review E, Vol. 62, No. 2, 2000, pp. 2428 - 2438.*
14. *Yekta-Fard, M., Ponter, A.B., 'Factors Affecting the Wettability of Polymer Surfaces', J.Adhesion Sci.Technol., Vol.6, No.2, 1992, pp.253 - 277.*
15. *Brochard-Wyart, F., Fondecave, R., 'Wetting Laws for Polymer Solutions', Europhysics Letter, Vol. 37, No. 2, 1997, pp. 115 - 120.*
16. *de Gennes, P.G., 'Wetting: Statics and Dynamics', Rev. Mod. Phys., Vol. 57, No. 3, Part 1, 1985, pp.828 - 865.*
17. *Brochard, F., 'Spreading of Liquid Droplets on Thin Cylinders: The 'manchon/droplet' transition', J.Chem.Phys Vol. 84, No. 8, 1986, pp. 4664 - 4672.*
18. *Kamath, Y., K., Chen, X., Neimark, A., 'Finish Film Stability and its Relevance to Slinging of Spin Finish to a Spinline', National Textile Center Annual Report: 1999, C98-P02.*
19. *Washburn, E. W., 'The Dynamics of Capillary Flow', The Physical Review, Vol. 17, No. 3, 1921, pp. 273 - 283.*
20. *Skinner, F. K., Rotenberg, Y., Neumann, A. W., Contact Angle Measurements from the contact Diameter of Sessile Drops by means of a modified Axisymetric Drop Shape Analysis, Journal of Colloid and Interface Science, Vol. 130, No. 1, 1989, pp. 25 - 33.*
21. *Bracke, M., Voeght, F., Joos, P., The Kinetics of Wetting: the Dynamic Contact Angle, Progress in Colloid and Polymer Science, Vol. 79, 1989, pp. 142 - 149.*
22. *Bacri, L., Brochard-Wyart, F., Droplet Suction in Porous Media, The European Physical Journal E, Vol. 9, 2000, pp. 87 - 97.*
23. *Koštáková, E., Pociūtė, M., Lukáš, D., 'The Radial Capillary', Strutex (Structure and Structural Mechanics of Textile Fabrics) 2003: proceedings of 10th International Scientific Conference, 2003, Liberec, Czech Republic, ISBN 80-7083-769-1.*

Received 21.11.2005 Reviewed 24.06.2006